J Supercond Nov Magn (2012) 25:841–846
DOI 10.1007/s10948-011-1359-2

ORIGINAL PAPER

Pseudo-gap and Vertex Correction of Electron–Phonon Interaction in High Transition-Temperature Superconductors

Wei Fan

Received: 28 September 2011 / Accepted: 7 November 2011 / Published online: 29 November 2011

Abstract The strong-coupling Eliashberg theory plus vertex correction is used to calculate the maps of transition temperature (T_c) in parameter-space characterizing superconductivity. Based on these T_c maps, complex crossover behaviors are found when electron–phonon interaction increases from weak-coupling region to strong-coupling region. The doping-dependent T_c of cuprate superconductors and most importantly the emergence of pseudo-gap region can be explained as the effects of vertex correction.

Keywords Electron–phonon interaction · Vertex correction · Eliashberg theory · Pseudogap · High transition-temperature superconductor

1 Introduction

The standard strong-coupling theory has no bound on transition-temperature T_c of superconductors [1–4]. Recently, the significant large second moments $\lambda\langle\omega^2\rangle$ of Eliashberg function $\alpha^2F(\omega)$ for cuprate superconductors are measured from the experiments of electron relaxation via pump-probe optical spectroscopy [5] means that there are strong electron–phonon interactions in cuprate superconductors. The Eliashberg functions extracted from the measurements of infrared optical conductivity [6] and ARPES spectrum [7] for cuprate superconductors predicted very strong electron–phonon interaction and very high T_c over the experimental values [6]. The T_c in mean-field approximation of Eliashberg theory is higher than experimental T_c. In the situation of very strong electron–phonon coupling, nonadiabatic effects of the electron–ion system will be so important that the electrons are dressed heavily by lattice vibrations and the conventional strong-coupling theory needs to be generalized to include the nonadiabatic effects or the vertex corrects beyond Migdal's theorem [8–10]. The behavior of crossovers when electron–phonon interaction evolving from the weak-coupling region to the strong-coupling region were found in different theoretical calculations [11–14]. These crossovers are expected to prevent T_c from infinitely increasing with electron–phonon interaction. If the electron–phonon interaction is the underlying pairing-mechanism for unconventional superconductors such as the cuprate superconductors, it should provide reasonable explanations of the pseudogap region and the dome-shape of doping dependent T_c in the doping-T_c phase diagram.

In our previous calculations of strong-coupling theory plus vertex correction [10, 15, 16], (1) we have predicted that the highest T_c of cuprate superconductors is close to 160 K consistent with the present record of cuprate superconductors [10], and (2) the up-limit of T_c for iron-based superconductors is about 90 K [10] with 34–35 K space left to increase T_c beyond the present record about 55–56 K [17]; (3) we have successfully explained the spatial anticorrelation between the energy gap and phonon energy for cuprate superconductor Bi2212 [15]; (4) we have also found that it is very difficult to realize a home-temperature superconductor in a high-pressure metal hydrogen and other hydrogen-rich materials [16] because of a very strong vertex correction (or nonadiabatic effects) induced by small electronic bandwidth and high phonon frequency.

In this paper, the T_c maps including the influences of vertex corrections are studied. Complex crossovers are found

W. Fan (✉)
Key Laboratory of Materials Physics, Institute of Solid State Physics, Hefei Institutes of Physical Sciences, Chinese Academy of Sciences, 230031 Hefei, People's Republic of China
e-mail: fan@theory.issp.ac.cn

on these T_c maps when the parameter λ of electron–phonon coupling increases from weak-coupling region to strong-coupling region. These crossovers are very close to the well-known $\lambda = 2$ at which the value of T_c reaches its maximum [1]. The pseudogap region in the phase diagram with the same topology as the phase diagram of doping-dependent T_c for cuprate superconductor is explained as the effects of vertex correction. The interplay of vertex correction and Coulomb interaction can suppress theoretical T_c to access experimental values [6].

2 Theoretical Formulas

The calculations of vertex corrections are greatly simplified under isotropic approximation because the electron–phonon interactions are included in the vertex corrections only by the functions of electron–phonon interaction λ_n defined as $\lambda_n = 2\int_0^\infty d\omega\alpha^2F(\omega)\omega/(\omega^2+\omega_n^2)$. When temperature is very close to T_c, the energy-gap equation [8, 10] is simplified to

$$\sum_{n'=-\infty}^{+\infty} K_{nn'}(\Delta_{n'}/|\omega_{n'}|) = 0, \tag{1}$$

with the kernel matrix expressed as

$$\begin{aligned} K_{nn'} &= [\lambda_{n-n'}B_{nn'} - \mu^* + C_{nn'}]a_{n'} - \delta_{nn'}H_{n'}, \\ H_{n'} &= \textstyle\sum_{n''=-\infty}^{+\infty}\left[\frac{\delta_{n'n''}|\omega_{n''}|}{\pi k_B T} + \lambda_{n'-n''}A_{n'n''}s_{n'}s_{n''}a_{n''}\right], \end{aligned} \tag{2}$$

where the parameters $A_{nn'} = 1 - V^A_{nn'}$, $B_{nn'} = 1 - V^B_{nn'}$, $s_n = \omega_n/|\omega_n|$, and $a_n = (2/\pi)\arctan(E_B/Z_n|\omega_n|)$. E_B is the effective band width of conducting electrons. In the calculation a_n, $Z_n \sim 1$ takes the value of normal state. The three parameters of vertex correction $V^A_{nn'}$, $V^B_{nn'}$ and $C_{nn'}$ have the form

$$\begin{aligned} V^A_{nn'} &= S\sum_{n''}\lambda_{n-n''}s_{n'+n''-n}s_{n''}a_{n'+n''-n}a_{n''} \\ V^B_{nn'} &= 2S\sum_{n''}\lambda_{n-n''}s_{n'+n''-n}s_{n''}a_{n'+n''-n}a_{n''} \\ C_{nn'} &= S\sum_{n''}\lambda_{n-n''}\lambda_{n'-n''} \\ &\quad \times s_{n'-n''+n}s_{n''}a_{n'-n''+n}a_{n''} \end{aligned} \tag{3}$$

with $S = \pi^2 k_B T/2E_B$. The Coulomb pseudopotential is defined as $\mu^* = \mu_0/(1+\mu_0\ln(E_B/\omega_0))$, where $\mu_0 = N(0)U$, $N(0)$ the density of state of normal state at Fermi energy, U the Coulomb interaction between electrons and ω_0 characteristic energy of typical phonon correlated to superconductivity. If the vertex corrections are ignored, three parameters $V^A_{nn'}$, $V^B_{nn'}$ and $C_{nn'}$ are all equal to zero and the kernel (2) of the energy-gap equation reduces to the general form without vertex correction [2] after some symmetrizations and simplifications. It is convenient that the $K_{nn'}$ matrix is symmetrized as in [2]. The Eliashberg functions $\alpha^2F(\omega)$ have the same approximation as in [18] and is expressed by

$$\alpha^2F(\omega) = \frac{c}{(\omega-\Omega_P)^2+(\omega_2)^2} - \frac{c}{(\omega_3)^2+(\omega_2)^2}, \tag{4}$$

if $|\omega - \Omega_P| < \omega_3$ and $\alpha^2F(\omega) = 0$ for others, where Ω_P is the energy of phonon mode, ω_2 the half-width of peak of phonon mode, and $\omega_3 = 2\omega_2$. The parameter of electron–phonon interaction is defined as $\lambda = 2\int_0^\infty d\omega\alpha^2F(\omega)/\omega$. In order to build the Ω_P–λ space, at first the Ω_P is fixed and different λ values are calculated by changing parameter c, and the next step is that Ω_P is changed to establish completed Ω_P–λ space. The full parameter space Ω_P–λ–μ^*–E_B is built by treating μ^* as an independent parameter. The constraints between different parameters are separately considered once the T_c map in the full parameter space is obtained by numerical calculations of the strong-coupling theory. Other details in our calculations can be found in [10, 16].

The parameter Ω_P/E_B measures the magnitude of the vertex correction in the perturbing calculation. In fact, Ω_P and E_B do not always appear as the combination of Ω_P/E_B. Generally, one changes and the other stays unchanged in our calculations. From an electron point of view, the vertex correction or nonadiabatic effect can be controlled by the effective bandwidth E_B; on the other hand, from an ion point of view, it can be controlled by the cutoff ω_0 of phonon energy or Ω_P in the Einstein model. In this work, the vertex correction is controlled by the effective band-width E_B within the range from 0.5 eV to 5 eV. The situation $E_B = \infty$ is equivalent to no vertex correction. According to (3), we can see that the smaller E_B means that the stronger vertex correction.

3 Results and Discussions

Figure 1(a, b, c) illustrate the evolution of T_c map on the λ–Ω_P plane with decreasing E_B. Figure 1(a) is the T_c map having been obtained in the previous work without considering vertex corrections [10]. When $E_B = 1.7$ eV, the large deformation of T_c map with strong vertex correction is shown in Fig. 1(b) near the well-known $\lambda = 2.0$ in the region of high phonon energy. With E_B decreasing to 1 eV further, the region with strong vertex correction rapidly expands and occupies a large part of parameter space with $\Omega_P > 80$ meV in Fig. 1(c). In the region $\Omega_P < 80$ meV, the T_c is strongly suppressed, however, there are no discontinuous changes of T_c or breaking of contour lines. An important result from the Fig. 1 is that T_c does not change with λ monotonously if phonon energy Ω_P is high enough. Figure 2(a) shows the changes of T_c with λ along two arrows A and B shown

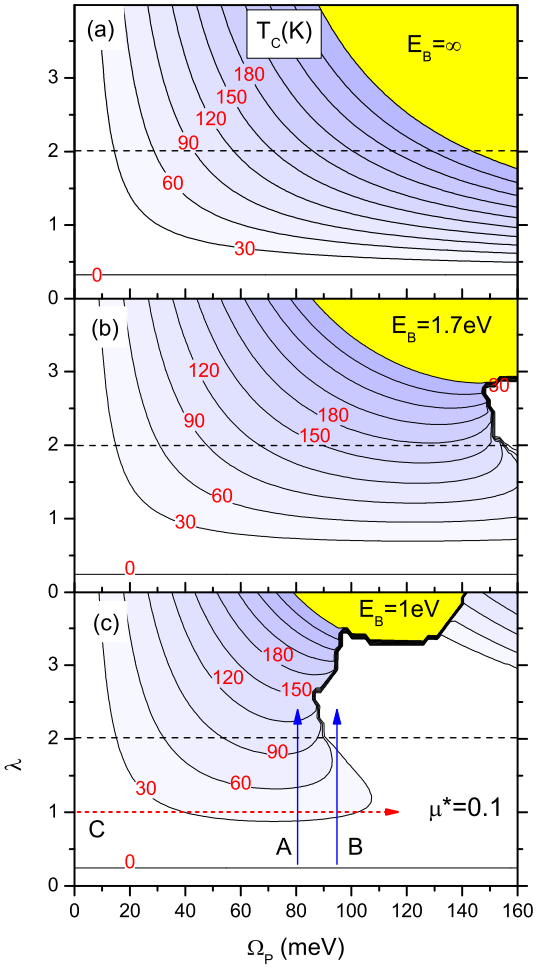

Fig. 1 The evolution of T_c map on λ–Ω_P plane with increasing strengths of vertex corrections (decreasing effective bandwidth E_B) with (**a**) $E_B = \infty$, (**b**) $E_B = 1.7$ eV, and (**c**) $E_B = 1$ eV. The Coulomb pseudopotential $\mu^* = 0.1$

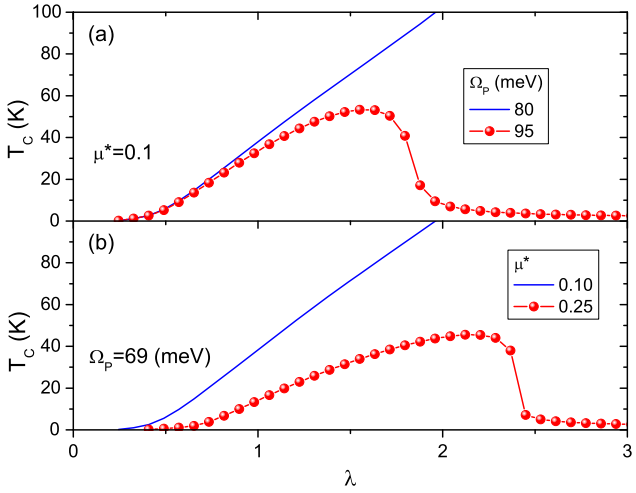

Fig. 2 (**a**) The T_c change along two arrows shown in Fig. 1(c) with fixed phonon energies $\Omega_P = 80$ meV and 95 meV, respectively. (**b**) The T_c change along two arrows shown in Fig. 3(c) with fixed Coulomb pseudopotentials $\mu^* = 0.10$ and 0.25, respectively

in Fig. 1(c). If $\Omega_P = 80$ meV, the T_c monotonously increases with λ. However, for $\Omega_P = 90$ meV, the T_c first increases with λ, reaches the maximum at $\lambda \sim 1.5$–1.7 and then quickly decreases with increasing λ. Further increasing $\lambda > 2$, T_c will be very low due to strong vertex corrections. The non-monotonous λ-dependent T_c in Fig. 2(a) had been found in the nonadiabatic theory of superconductivity [12]. Some crossover behaviors from weak coupling to strong coupling region had been predicted in the Holstein–Hubbard model solved numerically by the quantum Monte Carlo method [13] and in polaron theory [14]. It is very reasonable that the nonmonotonuos λ-dependent T_c is equivalent to the crossovers found in QMC calculation [13] and polaron theory [14]. So only the leading vertex correction can describe qualitatively very well the electron–phonon interaction in strong coupling region.

Figure 3(a) is the normal T_c map on μ^*–λ plane without vertex correction [10]. The figure shows that when $\mu^* > 0.2$, T_c is insensitive to the change of μ^*. The breaking contour lines with $T_c = 0$ K are because of the inaccurate calculations when $T_c < 0.1$ K if only $N = 200$ Matsubara energies are used. The contour lines with $T_c > 0.1$ K are accurate enough. If the Coulomb pseudo-potential and vertex correction work together, the situation will change drastically and some new interesting results will appear. The large deformations are found in Fig. 3(c) if E_B decreases to 1.0 eV. As expected, the large deformations and discontinuous changes of contour lines appear on the T_c map when $\mu^* > 0.20$. The contour lines with iso-values from $T_c = 20$ K to 200 K are bunched together within the rectangle region in Fig. 3(c) with $0.15 < \mu^* < 0.25$ and $\lambda > 2$. The figure clearly shows that if the Coulomb pseudopotential μ^* is large enough, the T_c will change with λ nonmonotonously. The changes of T_c along two arrows with $\mu^* = 0.1$ and 0.25 are plotted in Fig. 2(b). For $\mu^* = 0.25$, T_c first increases with λ until reaches the maximum at $\lambda = 2.2$ and then sharply decreases to smaller value at $\lambda = 2.5$. The crossover behavior is enhanced by strong Coulomb interaction.

The T_c map on E_B–λ plane is presented in Fig. 4(a) with $\Omega_P = 72$ meV. If E_B increases but λ keeps unchanged, the T_c monotonously increases with E_B until to the limit of non-vertex correction. More interestingly, on this map, the T_c is nonmonotonuos dependent on E_B along straight line from $P1$ to $P2$ companying by the decrease of λ from 5.0 to 0.2. The nonmonotonuos dependence of T_c on effective bandwidth E_B is equivalent to the band-filling effect of T_c. Our results show that, if $\Omega_P > 80$ meV, the suppression of T_c will be more prominently.

The values of T_c obtained from standard strong-coupling theory are generally higher than those measured in experiments. The copper-oxides superconductors $Bi_2Sr_2CaCu_2O_{8+\delta}$ and $Bi_2Sr_2Cu_2O_{6+\delta}$ studied in [6, 7] have very

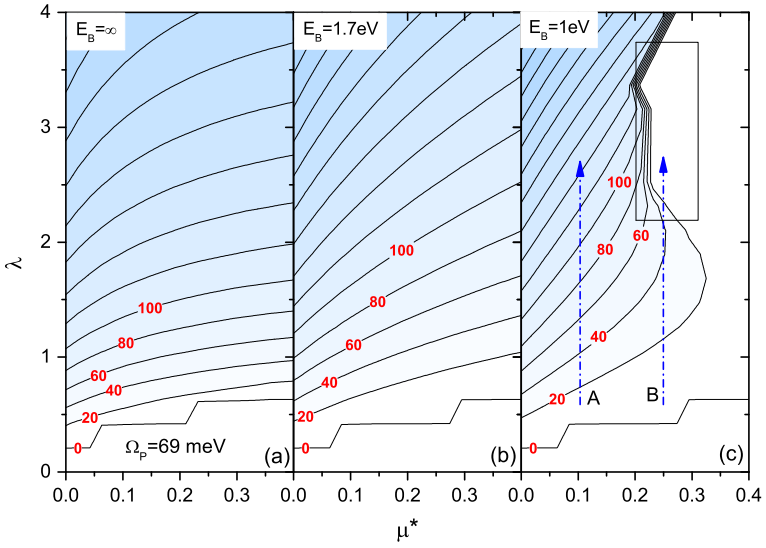

Fig. 3 The evolutions of T_c map on μ^*–λ plane ($\Omega_P = 69$ meV) with decreasing effective bandwidth (**a**) $E_B = \infty$, (**b**) $E_B = 1.7$ eV, and (**c**) $E_B = 1.0$ eV

strong electron–phonon interactions $\lambda \sim 2.36$–2.85 and overestimated T_c in underdoped samples. With increasing doping δ, the values of λ decrease to about 0.35–1.42 [6]. The effective bandwidths E_B of conducting electrons for these cuprates are distributed from 1 eV to 3 eV. The effective phonon energies are distributed from 50 meV to 80 meV. We recalculate the values of T_c along straight line $P1$–$P2$ in Fig. 4(a) under the assumption that the Coulomb interaction is strong in the underdoped region $\mu^* = 0.3$ at $P1$ and weak in the overdoped region $\mu^* = 0.1$ at $P2$. For simplicity, μ^* linearly decreases from 0.3 at $P1$ to 0.1 at $P2$. As shown in Fig. 4(b), if $\lambda < 4.0$, the values of T_c are reduced from around 200 K to lower than 150 K and close to experimental values [6]. In the strong-coupling region $4.0 > \lambda > 3.0$, T_c is very low. Our results provided an explanation to the pseudogap in underdoped region shown in Fig. 4(b). The cooper-pairs preform at T_c^* the transition temperature in mean field approximation on the standard strong-coupling theory. However strong nonadiabatic effects induce the instability of cooper-pairs and the real T_c has lower value. The T_c^* degenerating with T_c in the overdoped region is similar to the example (1) of Fig. 9 in [19]. The preformed cooper-pairs in cuprate superconductors are supported by measurements of Nernst effect [20], specific-heat [21], and many other methods.

An interesting result is that at very strong coupling $\lambda > 4.0$, the effects of vertex corrections superficially become weak. Even there are positive vertex correction that had been found in other work [12]. The electronic states in region *SP* with $\lambda > 4.0$ are strong-coupling pairs [22]. The Fig. 4(b) shows a crossover from BCS state to strong-coupling pairs state with increasing electron–phonon interaction λ. It's obviously that Fig. 4(b) has the same topology as the well-known T_c-doping phase diagram. It's dependent on whether the parameter λ electron–phonon interaction decreases with increasing doping or not. This point had been proved in recent experiments [6, 7]. The δ–λ curve in Fig. 4(c) is based on data in Ref. [6]. It's urged that there will be other experiments supporting this point.

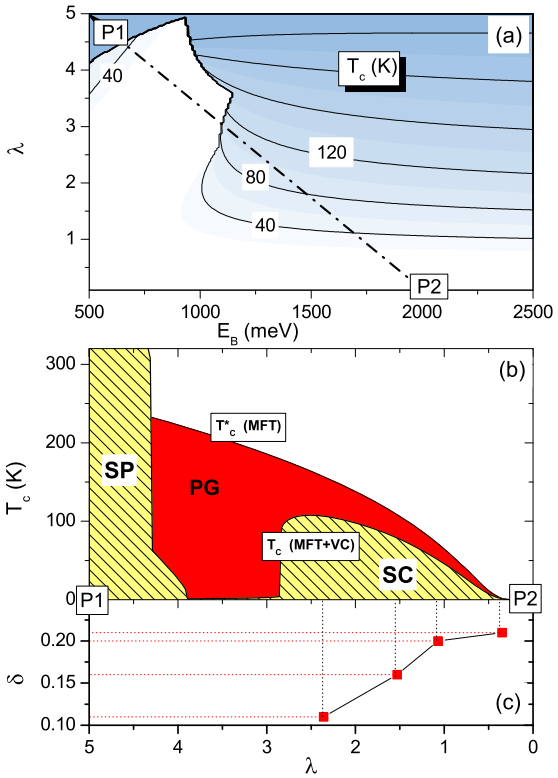

Fig. 4 (**a**) The T_c map on E_B–λ plane with $\mu^* = 0.25$ and $\Omega_P = 72$ meV. (**b**) The curve T_c (MFT + VC) is the evolution of T_c from $P1$ to $P2$ in (**a**) but μ^* linearly decreases from 0.3 to 0.1. The *solid curve* T_c^* (MFT) is the standard result in strong coupling theory without vertex correction. (**c**) The δ–λ relation is adopted in [6]

In order to analyze our results more deeply, we present individually the effects of nonadiabatic parameters $V^A_{nn'}$, $V^B_{nn'}$ and $C_{nn'}$ on T_c in Fig. 5(a). Equation (2) indicated that $V^B_{nn'}$ and $V^A_{nn'}$ are the renormalization to the parameter of electron–phonon interaction λ and $C_{nn'}$ is the renormalization to Coulomb pseudopotential μ^*. The T_c–λ curve labeled with V^B is calculated by allowing $V^B_{nn'} \neq 0$ and setting $V^A_{nn'} = 0$ and $C_{nn'} = 0$. Other curves are obtained with the same manner. We can find that the dome shape curve of T_c in the region $\lambda < 4.0$ is generated by the effects of $V^B_{nn'}$. In the region $\lambda > 4.0$, the effects of $V^A_{nn'}$ and $C_{nn'}$ cancel the effects of $V^B_{nn'}$ so that the strong coupling pairs in the mean field approximation are restored and even have a higher T_c. This fact can be clarified from the Fig. 5(b, c) in that the averages of the absolute values of diagonal and off-diagonal elements of parameter matrix $|A_{nn'}| = |1 - V^A_{nn'}|$, $|B_{nn'}| = |1 - V_{nn'}|$, and $|C_{nn'}|$ have larger changes mainly in the region $2.5 < \lambda < 4.0$. Moreover, in the region $\lambda > 4.3$, the $|A_{nn'}|$ and $|B_{nn'}|$ are close to normal values 1.0 just as in weak coupling region. Additionally, the average values of diagonal elements of the parameter matrix $|C_{nn'}|$ and $|B_{nn'}|$ steadily increase with λ and lead to positive vertex-correction.

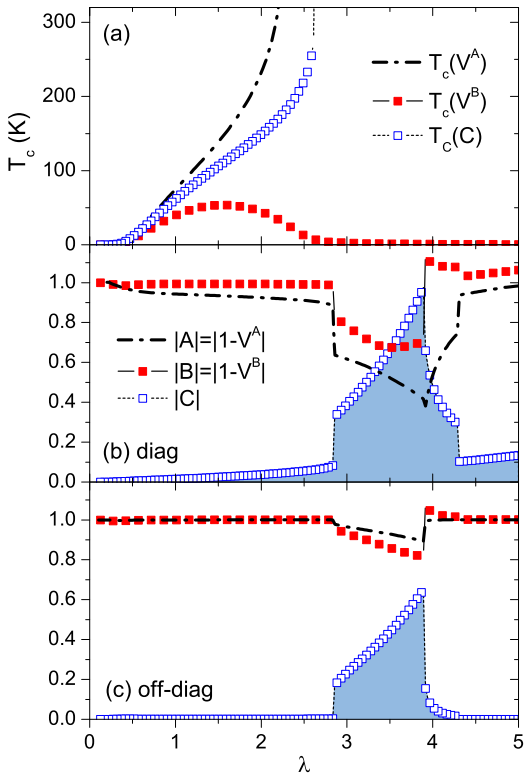

Fig. 5 (**a**) The effects of three nonadiabatic parameters $V^A_{nn'}$, $V^B_{nn'}$ and $C_{nn'}$ on T_c. (**b**, **c**) The changes of average values of diagonal and off-diagonal matrix elements of $|A_{nn'}| = |1 - V^A_{nn'}|$, $|B_{nn'}| = |1 - V^B_{nn'}|$ and $|C_{nn'}|$ with increasing λ

4 Discussion and Conclusion

The well-known Morel–Anderson relationship $\mu^* = \mu_0/[1 + \mu_0 \ln(E_B/\Omega_P)]$ that sets a constraint to parameter-space has only quantitatively influence on the T_c–E_B curve in Fig. 4(b). Figure 6(a) shows the T_c–E_B curves for different choices of $\mu_0 = 0.3$, 0.6, 1.2. We find that, for different μ_0, there are no significant changes of the maximum and minimum compared with the T_c–E_B curve with μ^* linear-dependent on E_B in Fig. 4(b). The underlying reason is that the strong-coupling effect of electron–phonon interaction is dominated over the Coulomb interaction in strong coupling region.

In the electron–phonon interaction theory, the coupling constant between electron and phonon is dependent on the phonon energy by $g = (\hbar/2MNV\omega)^{1/2}J$. There are feedback effects coming from the shift of phonon energy (or phonon self-energy). The Hopfield–McMillan relation $M\langle\omega^2\rangle\lambda = I = N(0)\langle J^2\rangle$, as the average effects of the feedback, is exact and nonperturbed and it can be taken as the role of sum-rule in electron–phonon interaction theory of

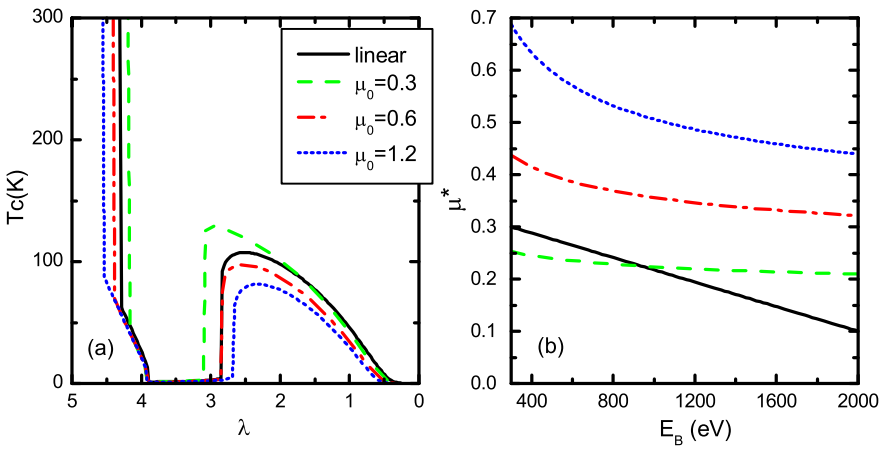

Fig. 6 (**a**) The curves of T_c evolute along the *straight line* from $P1$ to $P2$ in Fig. 4(a) with $\mu^* = \mu_0/(1+\mu_0 * \ln(E_B/\Omega_P))$. (**b**) The μ^*–E_B curves are plotted with $\mu_0 = 0.3$, 0.6 and 1.2, respectively. As a comparison, the curve in Fig. 4(b) with μ^* linearly dependent on E_B is plotted together

superconductivity. Based on the Hopfield–McMillan relation, the parameter of electron–phonon interaction is dependent on M and ω. In the McMillan's original paper, a maximum of T_c was found for fixed I if the Hopfield–McMillan relation was considered [1]. It is important that by using the Hopfield–McMillan relation the anomalous isotope effects with $\alpha > 0.5$ of fulleride and cuprate superconductors can be naturally explained as the effects of anharmonic vibrations of crystal lattice [23, 24]. The anticorrelation between phonon energy and the energy gap found in the cuprate superconductor is a very successful application of the Hopfield–McMillan relation [15]. One of our previous works had shown that, if there are no structure transitions under pressure, for simple metal, λ and ω approximately satisfy the Hopfield–McMillan relation with increasing pressure [25].

In summary, the nonmonotonuos changes of T_c with increasing λ show the crossover behaviors near $\lambda = 2$ when λ evolving from the weak-coupling region to a strong-coupling region. The crossovers can explain both the pseudogap phenomenon and the dome shape of doping dependent T_c of cuprate superconductors. The T_c maps in the previous paper [10] and the maps with vertex corrections in this paper provide a very comprehensive understanding of superconductivity of cuprate superconductors.

Acknowledgements The author thanks Prof. E. Cappelluti for very helpful discussions. The project was supported by the Knowledge Innovation Project of the Chinese Academy of Sciences.

References

1. McMillan, W.L.: Phys. Rev. **167**, 331 (1968)
2. Allen, P.B., Dynes, R.C.: Phys. Rev. B **12**, 905 (1975)
3. Allen, P.B., Mitrovič, B.: Theory Superconducting T_c. Solid State Physics, vol. 37. Academic Press, San Diego (1982)
4. Wu, H.S., Weng, Z.Y., Ji, G.D., Zhou, Z.F.: J. Phys. Chem. Solids **48**, 39 (1987)
5. Gadermaier, C., Alexandrov, A.S., Kabanov, V.V., Kusar, P., Mertelj, T., Yao, X., Manzoni, C., Brida, D., Cerullo, G., Mihailovic, D.: Phys. Rev. Lett. **105**, 257001 (2010)
6. van Heumen, E., Muhlethaler, E., Kuzmenko, A.B., Eisaki, H., Meevasana, W., Greven, M., van der Marel, D.: Phys. Rev. B **79**, 184512 (2009)
7. Ruiz, H.S., Badía-Majós, A.: J. Supercond. Nov. Magn. **24**, 1273 (2011). arXiv:1005.4770 [cond-mat]
8. Kostur, V.N., Mitrović, B.: Phys. Rev. B **50**, 12774 (1994)
9. Grimaldi, C., Pietronero, L., Strässler, S.: Phys. Rev. B **52**, 10530 (1995)
10. Fan, W.: Physica C **469**, 177 (2009)
11. Alexandrov, A.S.: Phys. Rev. B **38**, 925 (1988)
12. Paci, P., Cappelluti, E., Grimaldi, C., Pietronero, L.: Phys. Rev. B **65**, 012512 (2001)
13. Freericks, J.K., Jarrell, M., Scalapino, D.J.: Phys. Rev. B **48**, 6302 (1993)
14. Nasu, K.: Phys. Rev. B **42**, 6076 (1990)
15. Fan, W.: Chin. Phys. Lett. **25**, 2217 (2008)
16. Fan, W., Wang, J.L., Zou, L.J., Zeng, Z.: Chin. Phys. Lett. **27**, 087402 (2010)
17. Ren, Z.A., Lu, W., Yang, J., Yi, W., Shen, X.L., Li, Z.C., Che, G.C., Dong, X.L., Sun, L.L., Zhou, F., Zhao, Z.X.: Chin. Phys. Lett. **25**, 2215 (2008)
18. Scalapino, D.J., Schrieffer, J.R., Wilkins, J.W.: Phys. Rev. **148**, 263 (1996)
19. Norman, M.R., Pines, D., Kallin, C.: Adv. Phys. **54**, 715 (2005)
20. Xu, Z.A., Ong, N.P., Wang, Y., Kakeshita, T., Uchida, S.: Nature **406**, 486 (2000)
21. Wen, H.H., Wu, G., Luo, H.Q., Yang, H., Shan, L., Ren, C., Cheng, P., Yan, J., Fang, L.: Phys. Rev. Lett. **103**, 067002 (2009)
22. Chakraverty, B.K.: Nature **287**, 393 (1980)
23. Crespi, V.H., Cohen, M.L., Penn, D.R.: Phys. Rev. B **43**, 12921 (1991)
24. Fan, W.: Int. J. Mod. Phys. B (2011, in press). arXiv:0811.3813
25. Fan, W., Li, Y.L., Wang, J.L., Zou, L.J., Zeng, Z.: Physica C **470**, 696 (2010)